Journal of Civil Engineering (IEB), 51 (2) (2023) 121-129

Journal of Civil Engineering IEB

Modeling of shear stress distribution in artificial bend open channels

Aysha Akter and Md. Redwoan Toukir

Department of Civil Engineering,
Chittagong University of Engineering and Technology, Chittagong, Bangladesh

Received 10 November 2023

Abstract

By experimenting with an artificial bend channel, this study focuses on the flow pattern and other hydrodynamic changes in a meandering river portion. The changing pattern of the meandering properties can be understood through the shear stress distribution and other hydrodynamic characteristics. Furthermore, this comparative study can explain the comprehensive morphological characteristics of the present meandering portion of various rivers and describe the complete morphological attributes of the meandering part of different rivers. This study establishes an analytical validation of a numerical model with field-observed data of artificial bend channels and observes the other hydrodynamic characteristics by changing flow patterns through the model. While laboratory or field experiments involve time and cost, a validated numerical model can be an alternative solution to visualize and analyze different bending channel scenarios. In this study, Nays2D, the solver in the IRIC numerical model used for simulation. The Reynolds Shear Stress Extrapolation method could directly correlate the velocity with shear stress and determine shear stress distribution for three different planes among the various shear stress determination methods. So, the shear stress distribution from the field data was reasonably determined by this model. Thus, this model could provide relevant information to the other rivers.

Keywords: Artificial channel; meandering; shear stress; bend; numerical model.

1. Introduction

A meandering river portion's uneven shape and geometric pattern pose complex hydrodynamic and morphological characteristics. Higher velocities and erosion occur near the outer bank beyond the bend apex, while the inner bend point bar grows laterally towards the external bank, increasing the bending amplitude (Li et al., 2021). These dynamics maintain the meandering evolution, and shear stress is usually used as an indicator in fluvial studies to predict this evolution. Variables can analyze shear stress in the meandering river and explore shear stress in the meandering river, including sinuosity, the radius of curvature, and the meander wavelength (Uddin and Rahman, 2012; Li et al., 2021). Alongside erosion and

deposition, bed shear stress of the river can also affect the hydraulic structure that builds in the river bed (Jia et al., 2010; Kumar Das et al., 2020). Generally, the meandering river is subjected to erosion and deposition, and the presence of bends is of difficult contribution to this. So far, no experimental study has been conducted entirely to understand the phenomena of bed shear stress in the meandering bends curves in the context of rivers in Bangladesh. There are many meandering portions of the Karnafuli River situated in Chittagong (Das et al., 2014; Akter et al., 2018; Akter and Dayem, 2020). Figure 1 shows some parts of the meandering portion of the Karnafuli and Halda rivers, bending angles. An artificial bending channel experiment setup would be helpful in understanding the flow morphology of these portions of the river. The required modification of waterways, the diversion of flow, construction of shipping facilities, and controlling pollution system, rivers bend needs to be studied in different aspects. However, the processes governing the velocity redistribution in sharp meander bends are still poorly understood, primarily attributed to most meander models' validity range and the scarcity of experimental data. Intensive experimental studies on meandering bends are in urgent need in this connection. This reported study aimed to compute shear stress based on laboratory data collected in a 3D flow field, determine shear stress changes due to bends, and correlate them with geometric features.

2. Materials and methods

Shear stress in a meandering channel can be better described and zed by planimetric variables, including sinuosity of 1.5 or greater, the radius of curvature, amplitude of meander, meander wavelength, channel top width, and total angle of the bend (Biswas and Barbhuiya, 2018; Kumar Das et al., 2020). In the bends, pressure gradients and centrifugal forces combine to produce transverse circulations and secondary flows resulting in 3D helical flow patterns. The secondary flows in river bend result from different velocities between the surface and bed, centrifugal force, and friction between sides and walls (Wang et al., 2019). Then, velocity vectors in the stream-wise direction coupled with transverse vectors resulting from secondary circulation cause variations in boundary shear stress. Thus, shear on the outer bank is more significant than shear on the inner bank due to super-elevation and the locally steep downstream energy gradient. In conjunction with the previous investigation on shear stress and velocity distributions in trapezoidal meandering bends with varying entrance conditions, Ippen and Drinker extended the range of stream parameters (I. et al., 2012) This study concluded that boundary shear stress patterns obtained could not be predicted quantitatively from the gross characteristics of flow (I. et al., 2012)—a relationship between relative curvature and maximum relative shear stress needed to be determined. As per the published report, the United States Bureau of Reclamation (USBR) reported shear stress and velocity distributions in a single trapezoidal bend to determine optimal channel cross-sections to stabilize earthen canals (Ramsis, 1995). Later on, USBR reported on field data acquisition for meandering bends.

2.1 Theory

Many researchers suggested different methods for determining shear stress in the meandering channel. Famous methods for the wide-open channel flume with required instruments are (i) the Preston tube method, (ii) linear regression of the flow velocity profile, (iii) Rozovskii method, and (iv) Reynolds shear stress extrapolation. Preston (1954) performed a laboratory study to determine turbulent skin friction using Pitot tubes. The linear regression of the flow velocity profile method for shear stress calculation is based on the relationship between the logarithmic profile of flow depth and flow velocity. Clauser (1956) obtained shear stress by rearranging the relation between shear velocity and velocity. Also, Afzalimehr and Anctil (2000) explained that combining the wall law with the respected equation can obtain shear stress (Fzalimehr and Anctil, 2000). The Rozovskii method is for the computation of radial

shear stress by using equations that were derived from Cartesian coordinates. Rozovskii introduced the equations for analyzing the flow characteristics in a meandering channel. In addition, Rozovskii (1961) provided a comparison and discussion of other researchers' studies since the introduction of the radial shear stress calculation method in meandering channels (Rozovskii and Prushansky, 1957). Julien (1998) explained that internal and external forces form the Cartesian component of the fluid. Internal forces apply at the center of the mass (Julien, 2010). Stress can be classified as two other components in external forces: (i) normal stress and (ii) tangential stress. The study focuses on the calculation of the tangential stress that corresponds with the Reynolds shear stress comprised of six different components: $\tau_{xy} = \tau_{yx}$, $\tau_{yz} = \tau_{zy}$, and $\tau_{zx} = \tau_{xz}$. To calculate six components of the Reynolds shear stress, an Acoustic Doppler Velocimeter (ADV) was used in this study. The representative flow data from the ADV are covariance (*COV*) because they are directly used to obtain the Reynolds shear stress. As shown in Figure, the flow velocity is not always identical to the average flow velocity due to the turbulence in the flow. The basic concept of covariance in this study is the correlation of two components of flow velocity out of three flow velocity components: *Vx*, *Vy*, and *Vz* Reynolds shear stress extrapolation using ADV data (Wahl, 2000) could be calculated as:

$$\tau_{xy} = \tau_{yx} = -\rho \times (COV - XY) \tag{1}$$

Where,
τ_{xy} = turbulent shear stress that applies along the *y*-axis and is caused by flow velocity fluctuation in the direction of the *x*-axis
τ_{yx} = turbulent shear stress that involves along the *x*-axis and is caused by flow velocity fluctuation in the direction of the *y*-axis
ρ = mass density of water
COV-XY = covariance of two variables.
COV-XY is the covariance of two variables (*Vx* and *Vy*). The applicable equation is as:

$$COV - XY = \frac{\sum V_x V_y}{n-1} - \frac{\sum V_x \sum V_y}{n(n-1)} \tag{2}$$

where
Vx = flow velocity along the *x*-axis
Vy = flow velocity along the *y*-axis and
n = number of samples that collected velocity data

For the extrapolation of the experiment, a numerical model was used for further analysis. IRIC was used for this purpose. The data represent boundary conditions, including bathymetry and water discharges for the study. The research set two boundary conditions: the upstream portion of the channel and the other is on the downstream part. In the first interpretation step, all the relevant physical processes identified in the prototype are translated into governing equations compiled into the mathematical model. A mathematical model, therefore, constitutes the first approximation to the problem. Then, a solution step is required to solve the mathematical model. The numerical model embodies the numerical techniques used to solve the governing equations that form the mathematical model. Another solution step involves the solution of the numerical model in a computer and provides the modeling results. This step embodies further approximations and simplifications, i.e., those associated with unknown boundary conditions, imprecise bathymetry, unspecified water and or friction factors, etc. Finally, the data is supposed to be interpreted and placed in the appropriate prototype context. This last step closes the modeling cycle and ultimately identifies the problem that drives the modeling efforts.

On the other hand. Nays 2D is a computational model for simulating hydrodynamic characteristics in an open channel. It solves the continuity and momentum equations, for water flow transforms from the Cartesian coordinate system to a moving boundary-fitted coordinate system (Chang-Lae and Yasuyuki, 2005). In this study, the IRIC model was conducted with a Nays2DH solver. The model has calculated its hydrodynamic features based on this 2D solver.

2.2 Experimental setup

The cross-section of the artificial channel is 10m × 0.75m × 0.75m. The shape of the channel is rectangular. There are two bending portions on the channel, and these were 90°and 130° individually. A sluice gate with a controlling valve was located at the start of the channel. The flow on the channel was controlled through a 0.075m or 75 mm pipe, and the drainage facility completely depends on the gravitational forces. The bed and wall surface of the channel was built with a concrete structure. Figures 2 a and b describe the schematic diagram of the channel. For the experimental setup, the channel was ignored up to 1m from the upstream to avoid turbulence effects. There is a sluice gate at the upstream part of the channel, and downstream of the channel, there was a barrier of different heights to maintain different water levels for the experiment. A rectangular weir was used to maintain a certain water level. The data of hydrodynamic features such as velocity and the water level had been acquired with 0.5 m. The velocity data were collected from the ADV, and the water level data were obtained by meter gauge in every cross-section. The ADV probe was set vertically downward to the face of the water surface under 60% of the depth of water from its surface.

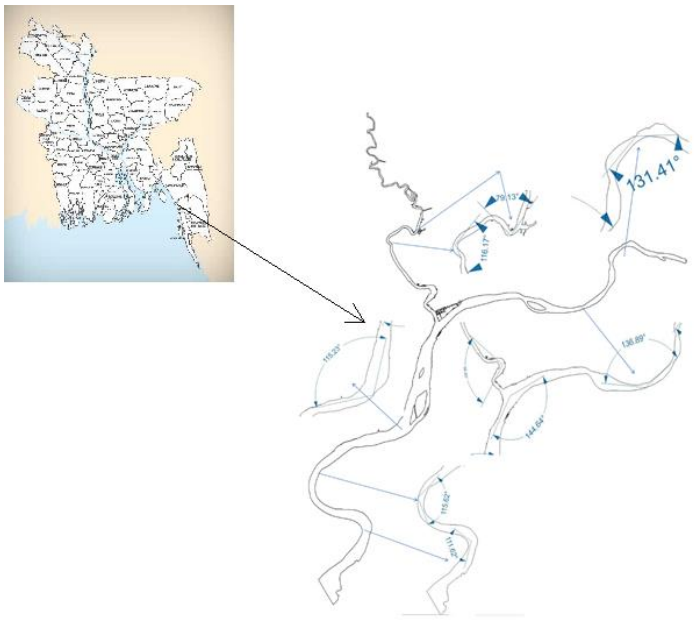

Fig. 1. Meanderings in the Karnafuli and Halda River.

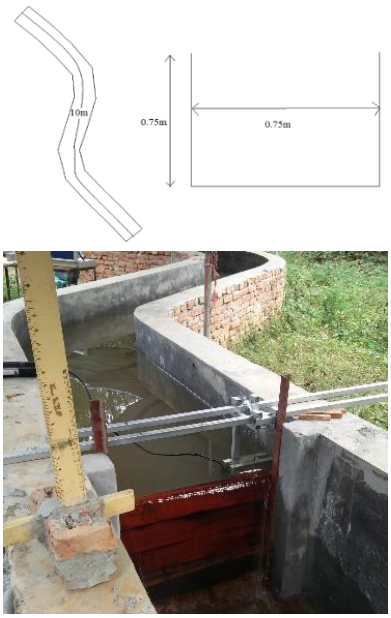

Fig. 2. Experimental bending channel setup

2.3 Model setup

The specific algorithm was selected to generate a grid in IRIC and the hydrodynamic equations were applied. The centreline of the channel was passed through the grid of 11×9 cells. The created grid has 99 nodes (Figure 3). In the model, the grid requires elevation data for every node to complete the elevation profile of the study area. The elevation data acquired from the survey during the field experiment was inputted into the nodes (Figure 4). Their

hydrodynamic characteristics set the boundary condition of two sections (upstream and downstream). The simulation was based on uniform flow conditions, and the downstream portion-maintained free-fall conditions for simulation.

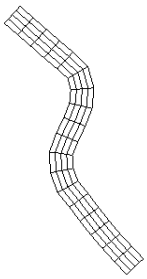

Fig. 3. Grid generation by IRIC grid algorithm.

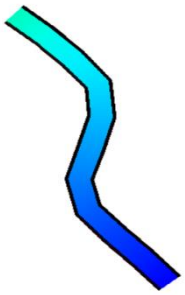

Fig. 4. Bird's eye view of the elevation profile.

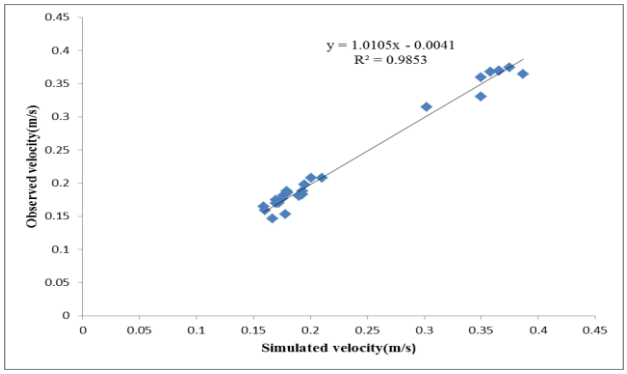

Fig. 5. Simulated and observed velocity.

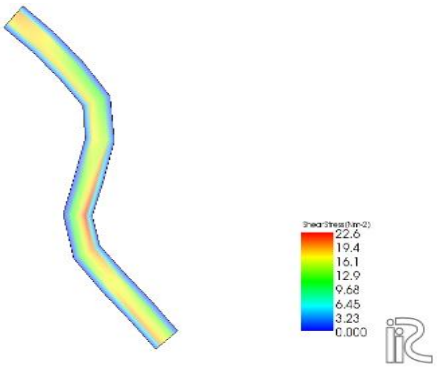

Fig. 6. Shear stress distribution for 15 l/s flow

3. Results

The experiment was conducted by ADV and adopted Wahl's Formula based on Reynold's Shear stress extrapolation. Shear stress on the XY plane is the section's bed shear stress, and the remaining shear stress on XZ and YZ planes is the boundary shear stress in the two different directions. Flow in a channel is a factor for shear stress distribution. With the various level of flow, the shear stress distribution in the channel can be optimized. Firstly, a specific flow condition was established in the channel.

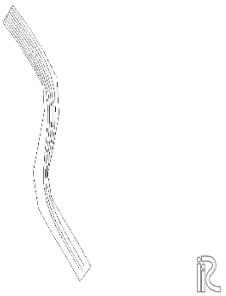

Fig. 7. Streamline profile for 12 l/s flow.

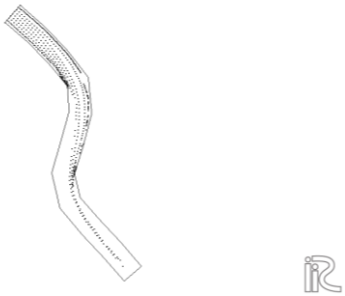

Fig. 8. Particle distribution for 12 l/s flow in the channel.

The model is validated with the field observed value. The model trained with the different flows to follow the shear stress distribution with an additional value. Then, the model was validated with the same calibration parameter and set up for both high flow (15 l/s) and low

flow (2 l/s). A low flow of 2 l/s was introduced through the channel's inlet (Appendix). Velocity distribution and water level at different points were measured continuously.

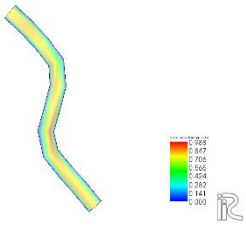

Fig. A1. Velocity distribution for 12 l/s flow.

Fig. A2. Shear stress distribution for 12 l/s flow.

Fig. A3. Velocity distribution for 15 l/s flow

Fig. A4. Shear stress distribution for 15 l/s flow.

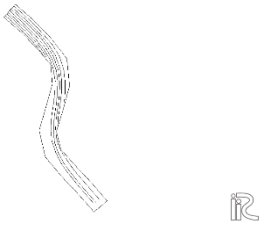

Fig. A5. Streamline profile for 2 l/s flow.

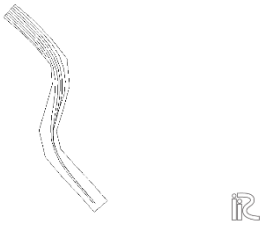

Fig. A6. Streamline profile for 5 l/s flow.

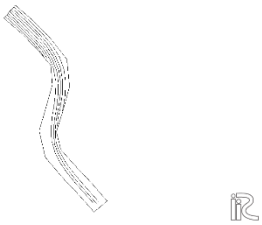

Fig. A7. Streamline profile for 10 l/s flow

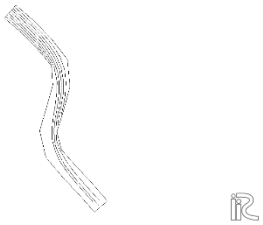

Fig. A8. Streamline profile for 12 l/s flow

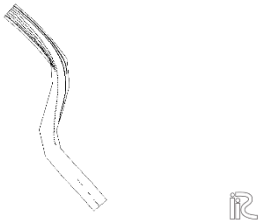

Fig. A9. Particle distribution in the channel during 2 l/s flow.

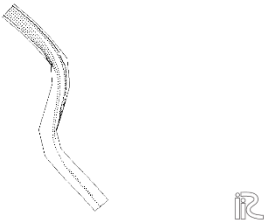

Fig. A10. Particle distribution in the channel during 8 l/s flow.

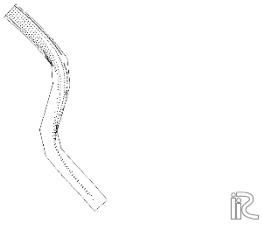

Fig. A11. Particle distribution in the channel during 12 l/s flow.

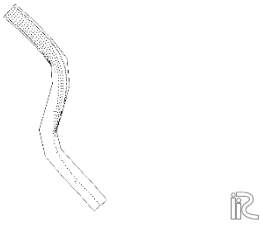

Fig. A12. Particle distribution in the channel during 15 l/s flow.

It was essential to maintain the flow constantly. So, the discharge value through the inlet pipe was observed simultaneously from the flow meter. Also, the experiment had 15 l/s discharge during the high flow experiment. The velocity distribution map shows the velocity is higher in the middle section of the channel. The observed velocity near the boundary section is much lower than the middle section. The left and the right boundary have almost the same velocity in the straight portion, while an uneven velocity distribution was observed in the bending portion. This is the common scenario for both high and low flow conditions. For validating the model with observed data Manning's Roughness coefficient (n) was considered a calibration parameter. An 'n' value of 0.029 was deemed feasible for this study. Figure 5 concludes the correlation between simulated and observed velocity.

Different discharge in the upstream boundary leads to other hydrodynamic characteristics. In this study, shear stress, velocity, streamline, and particle distribution for additional flow are the topics of interest. The different scenario shows shear stress and velocity have a proportional relation. Generally, the region with higher velocity has higher shear stress (Figure 6). With the increase of flow and velocity, the shear stress also increases, but the distribution pattern for every flow condition is almost identical. The inner bend portion possesses more shear stress and acceleration than the outer portion of the bend. With the increase of flow and velocity, the fluid particles move towards the concave portion of the bending. Still, it is the convex portion where materials accumulate most for sedimentation. From the flow's streamlined profile, the flow pattern influences the channel's first bending portion. As it was a rigid bed experiment, the erosion scenario was absent from the site, but particle distribution by the flow shows accumulation into the convex portion for both bends. The streamlined profile provides the flow characteristics to understand the flow characteristics for each flow distribution. With the increase of flow and velocity, the fluid particles move towards the concave portion of the bending. Still, it is the convex portion where materials accumulate most for sedimentation. From the streamlined profile of the flow (Figure 7), the flow pattern influences the first bending portion of the channel more. As it was a rigid bed experiment, the erosion scenario was absent from the site, but particle distribution by the flow shows accumulation into the convex portion for both bends (Figure 8). The flow pattern was well disturbed in the convex portion of the 1st bend, and flow took the more significant path to travel to the concave amount of the bend. For every flow condition, particles accumulate in the inner bend portion while the particle moves away with the flow from the outer bend. After crossing the first bend, the flow pattern flows the most straightforward approach that affects the second bend. The velocity profile suggests that next to the outer portion of the first bend tends to have more velocity than the inner portion of the second bend, which leads the flow to travel more frequently to the convex portion than the concave portion. The particles gather more into the convex part of the second bend.

4. Conclusions

Understanding the hydrodynamic characteristics in bending channels is always a challenging issue. This study aimed to establish a different scenario for shear stress and other hydrodynamic characteristics with varying flow conditions. This study paved the way for further experiments on morphodynamic and hydrodynamic characteristics in bending channels. The methodology for this study was to calibrate and validate a hydrodynamic model with applicable flow conditions and use the calibrated model for different flow scenarios. The model outcome validates the field observed data for high and low flow conditions. The different flow pattern imposed on the model was between these validated high and low flow values. Because of the lack of flow distribution facility in the field, it was best to co-relate a numeric model with a field study and move forward with the model. This research facility can be used for an experiment like bed deformation, the effect of wave or current, local scouring,

and sediment transport in bending channels. Throughout this research, the limitations that have been faced or should be improved are:

- An increase in flow in the inlet is needed. The velocity distribution in the channel needs to be higher to conduct a smooth morphological experiment;
- The experiment was carried out on rigid bed conditions. Scouring, deformation, and many other phenomena because of shear stress were absent from this setup;
- Other methods of shear stress determination could not be adopted for limited experimental instruments and facilities; and
- The effect on shear stress because of turbulent flow was not examined due to the absence of high flow.

Acknowledgments

The Department of Civil Engineering at Chittagong University of Engineering and Technology (CUET), Bangladesh has funded this study (titled: Investigation of Shear Stress in an Artificial Bend open Channel (ISSABC), CUET/DRE/2019-20/CE/033). Logistic supports from the BWDB are also appreciated.

References

Akter, A. Toukir, M. R., Das, N., Ismawi (2018) 'Hydrodynamic simulation of a selected reach in a tidal river', in IET Conference Publications. doi: 10.1049/cp.2018.1607.

Akter, A. and Dayem, A. (2020) 'Mapping river bathymetry using Stumpf model. IABSE-JSCE Conference on Advances in Bridge Engineering-IV-Definitive Outcomes for the People, 26-27 August 2020, Dhaka, Banglades', in.

Biswas, P. and Barbhuiya, A. K. (2018) 'Countermeasure of river bend scour using a combination of submerged vanes and riprap', International Journal of Sediment Research, 33(4), pp. 478–492. doi: https://doi.org/10.1016/j.ijsrc.2018.04.002.

Chang-Lae, J. and Yasuyuki, S. (2005) 'Numerical Simulation of Relatively Wide, Shallow Channels with Erodible Banks', Journal of Hydraulic Engineering. American Society of Civil Engineers, 131(7), pp. 565–575. doi: 10.1061/(ASCE)0733-9429(2005)131:7(565).

Clauser, F. H. (1956) 'The Turbulent Boundary Layer**The research presented in this article was supported by the Office of Scientific Research, A.R.D.C.; U. S. Air Force, under contract AF 18(600)671. The author was assisted by his colleagues Drs. S. Corrsin, G. Corcos, and D.', in Dryden, H. L. and von Kármán, T. B. T.-A. in A. M. (eds). Elsevier, pp. 1–51. doi: https://doi.org/10.1016/S0065-2156(08)70370-3.

Das, R., Hossen, M. B. and Akter, A. (2014) 'Predicting Bankline Changes in the Karnafuli River Using ARCGIS. In proceedings of the 2nd International Conference on Civil Engineering for Sustainable Development (ICCESD-2014), 14~16 February 2014, KUET, Khulna, Bangladesh, ISBN: 978-984-33-6373-2. pp.', in.

Fzalimehr, H. and Anctil, F. (2000) 'Accelerating shear velocity in gravel-bed channels', Hydrological Sciences Journal. Taylor & Francis, 45(1), pp. 113–124. doi: 10.1080/02626660009492309.

Thornton, C. I., Ursic, M. E., Baird, D. C., Sin, K.-S., Abt, S. R. (2012) 'Evaluating Boundary Shear Stresses in Natural-Shaped Channel Bendways', World Environmental and Water Resources Congress 2012. (Proceedings), pp. 1366–1375. doi: doi:10.1061/9780784412312.137.

Jia, D., Shao,X. , Wang, H., Zhou, G. (2010) 'Three-dimensional modeling of bank erosion and morphological changes in the Shishou bend of the middle Yangtze River', Advances in Water Resources, 33(3), pp. 348–360. doi: https://doi.org/10.1016/j.advwatres.2010.01.002.

Julien, P. (2010) 'Erosion and Sedimentation', Cambridge: Cambridge University Press. doi: 10.1017/CBO9780511806049.

Das, V. K., Barman,K., Roy, S., Chaudhuri, S. Debnath,K. (2020) 'Near bank turbulence of a river bend with self similar morphological structures', CATENA, 191, p. 104582. doi: https://doi.org/10.1016/j.catena.2020.104582.

Li, Z., Yang,H., Xia,J., Zhou, M., Deng, S. Wang,Y. (2021) 'Channel morphologic processes of a highly sinuous bend approaching neck cutoff by bank erosion in the middle Yangtze River', International Journal of Sediment Research, 36(4), pp. 457–467. doi: https://doi.org/10.1016/j.ijsrc.2021.01.001.

Ramsis, F. Y. (1995) 'Boundary Shear in Curved Channel with Side Overflow', Journal of Hydraulic Engineering. American Society of Civil Engineers, 121(1), pp. 2–14. doi: 10.1061/(ASCE)0733-9429(1995)121:1(2).

Rozovskii, I. L. and Prushansky, Y. T. (1957) 'Flow of water in bends of open channels', in.

Uddin, M. N. and Rahman, M. M. (2012) 'Flow and erosion at a bend in the braided Jamuna River', International Journal of Sediment Research, 27(4), pp. 498–509. doi: https://doi.org/10.1016/S1001-6279(13)60008-6.

Wahl, T. L. (2000) 'Analyzing ADV Data Using WinADV', (1), pp. 1–10.

Wang, J. Chen, L., Zhang, W., Chen, F. (2019) 'Experimental study of point bar erosion on a sand-bed sharp bend under sediment deficit conditions', Sedimentary Geology, 385, pp. 15–25. doi: https://doi.org/10.1016/j.sedgeo.2019.03.008.